Pure Appl. Geophys. 177 (2020), 1639–1657

https://doi.org/10.1007/s00024-019-02390-2

Pure and Applied Geophysics

The 1674 Ambon Tsunami: Extreme Run-Up Caused by an Earthquake-Triggered Landslide

Ignatius Ryan Pranantyo[1] and Phil R. Cummins[1]

Abstract—We present an analysis of the oldest detailed account of tsunami run-up in Indonesia, that of the 1674 Ambon tsunami (Rumphius in Waerachtigh Verhael van de Schuckelijcke Aerdbebinge, BATAVIA, Dutch East Indies, 1675). At 100 m this is the largest run-up height ever documented in Indonesia, and with over 2300 fatalities even in 1674, it ranks as one of Indonesia's most deadly tsunami disasters. We consider the plausible sources of earthquakes near Ambon that could generate a large, destructive tsunami, including the Seram Megathrust, the South Seram Thrust, and faults local to Ambon. We conclude that the only explanation for the extreme run-up observed on the north coast of Amon is a tsunami generated by an earthquake-triggered coastal landslide. We use a two-layer tsunami model to show that a submarine landslide, with an approximate volume of 1 km^3, offshore the area on Ambon's northern coast, between Seith and Hila, where dramatic changes in coastal landscape were observed can explain the observed tsunami run-up along the coast. Thus, the 1674 Ambon tsunami adds weight to the evidence from recent tsunamis, including the 1992 Flores, 2018 Palu and Sunda Strait tsunamis, that landslides are an important source of tsunami hazard in Indonesia.

Keywords: Eastern Indonesia, Ambon, tsunami hazard, landslide.

1. Introduction

Eastern Indonesia, and the Banda Sea in particular, is a region of very active and complex tectonics (Hamilton 1979; McCaffrey 1988; Spakman and Hall 2010; Pownall et al. 2013). Despite a historical record rich in major, destructive earthquakes and tsunamis, during the more recent era of instrumental seismology most of the major events have occurred in western Indonesia. The only way to better understand the tsunami threat in eastern Indonesia is therefore to glean as much information as we can from the historical record, which often consists of accounts that are sparse and difficult to interpret.

The oldest detailed tsunami account in Indonesia was documented by Rumphius (1675). A devastating earthquake rocked Ambon and its surrounding islands on 17 February 1674. The earthquake was followed by a massive tsunami about 100 m in run-up height which was only observed on the northern coast of Ambon Island while other areas experienced only minor tsunamis. The earthquake and tsunami caused more than 2300 fatalities, mostly on the northern shore of Ambon.

The source of the tsunami and earthquake is unknown. Løvholt et al. (2012) and Harris and Major (2017) speculated that it was triggered by an earthquake from south of Ambon and a landslide triggered by an earthquake from inside Ambon Bay, respectively. However, no attempt has been made to investigate this event further, particularly to answer why the extreme run-up was observed only on the northern coast of Ambon. Therefore, the primary source of the tsunami and earthquake remains open to question.

In the following sections of this paper, the tectonic setting around Ambon is discussed first, followed by our interpretation of the accounts of this event. The primary source of the earthquake and tsunami is investigated through analysis of the Rumphius document. Tsunami modelling is then performed to confirm the analysis. Lastly, the result of the analysis and the implications of the findings are discussed.

2. Tectonic Setting Around Ambon

Ambon is a small volcanic island that lies southwest of Seram Island (Fig. 1). It consists of two small

[1] Research School of Earth Sciences, Australian National University, Canberra, Australia. E-mail: ryan.pranantyo@anu.edu.au; phil.cummins@anu.edu.au

islands, Hitu and Leitimor, which are connected by a short isthmus (Fig. 2). Ambon is located to the southwest of Seram Island which is part of the outer Banda Arc. The islands are surrounded by major faults, namely the Seram Megathrust, Kawa Fault and the Banda Detachment (Fig. 1).

As summarised in Patria and Hall (2017), the Seram Megathrust stretches from Kai Islands in the east side to the northwest of Seram Island (Fig. 1). It is often described as a subduction zone (e.g. Hamilton 1979; Honthaas et al. 1998). However, others have argued that it is a foredeep produced by loading from a developing fold and thrust belt (Audley-Charles et al. 1979; Pairault et al. 2003; Spakman and Hall 2010). Through high-resolution bathymetry and seismic data, Patria and Hall (2017) confirmed the second hypothesis: that it is a result of oblique intra-plate convergence.

The Kawa Fault is a prominent structure in central Seram Island (Fig. 1). The fault runs from Piru Bay, off the northern shore of Ambon, to the central south of the island on the northern side of the Banda Sea. The fault has a major left-lateral movement identified through geological observations (Pownall et al. 2013). A large earthquake which caused a catastrophic tsunami on Seram Island in 1899 was suspected to have ruptured the Kawa Fault (Soloviev and Go 1974).

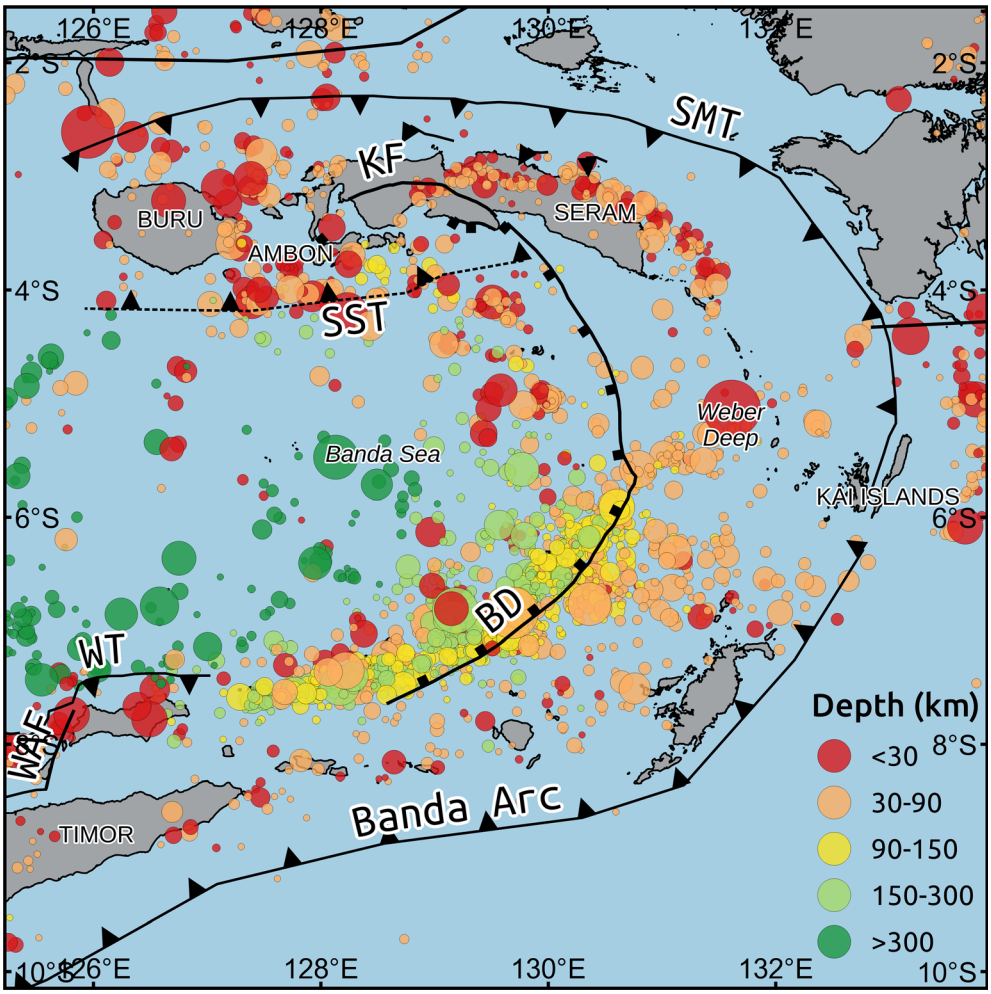

Figure 1
Tectonic setting of Ambon and its surrounding islands; *SMT* Seram Megathurst, *KF* Kawa fault, *SST* purported South Seram Thrust, *BD* Banda Detachment, *WT* Wetar thrust, *WAF* Wetar-Atauro fault

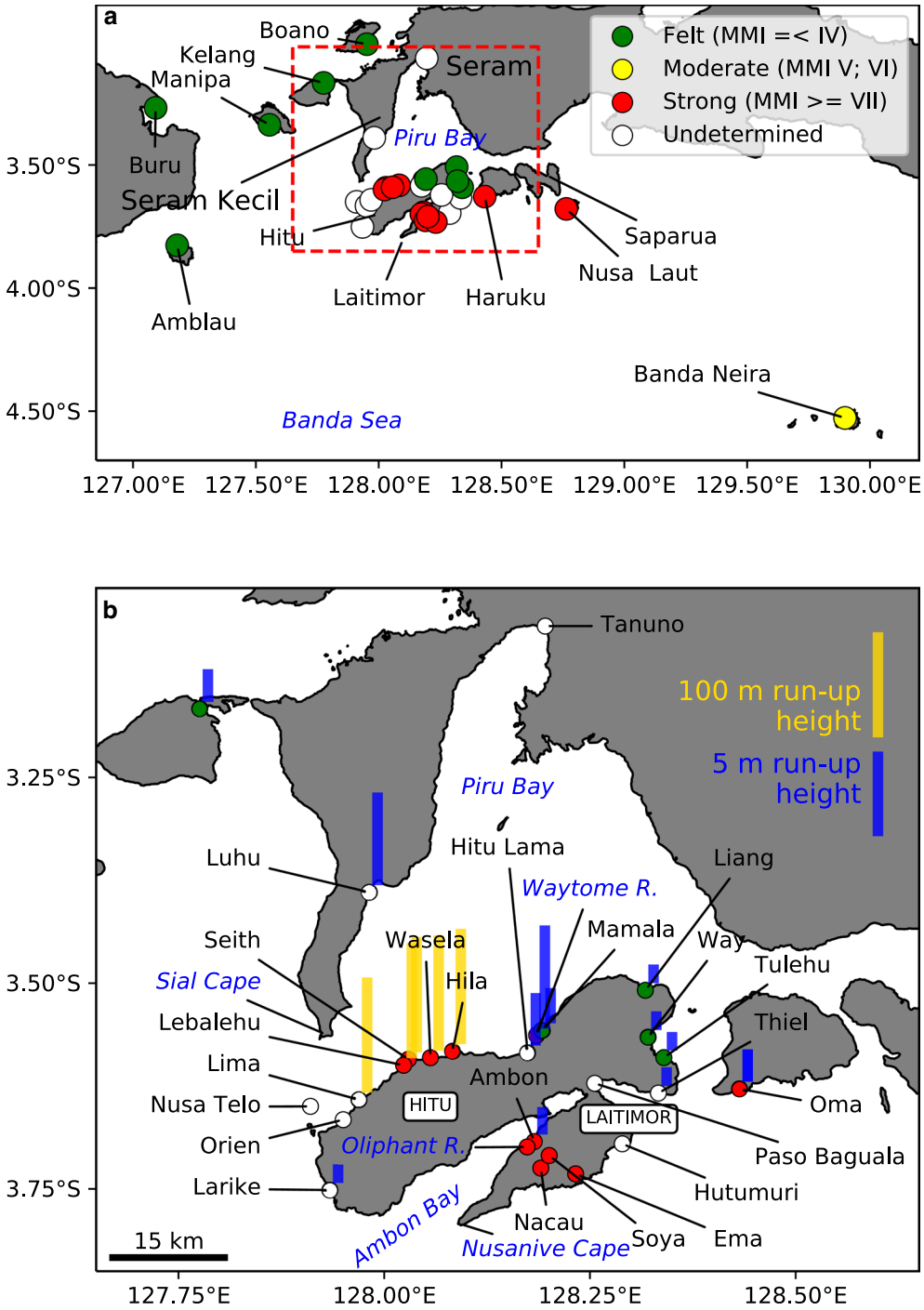

Figure 2
Historical accounts of the 1674 Ambon Island **a** earthquake and **b** tsunami. Location of map b is shown as the red dashed box. Colour circles represent interpreted earthquake intensity. Tsunami heights are indicated by the gold (100 m) and blue (5 m) color bars

At the southern end of Seram, Pownall et al. (2016) argue that the Kawa Fault continues to the Banda Sea and is related to the Banda Detachment (Fig. 1). The Banda Detachment is a recently discovered low-angle normal fault identified from geological observations and high-resolution

bathymetry data. Moreover, the Banda Detachment exhibits rapid extension as indicated by a very thin sediment layer in the Weber Deep (Pownall et al. 2016).

On Ambon, Watkinson and Hall (2017) identified several faults via a digital elevation model of the Shuttle Radar Topography Mission (SRTM). First, a normal fault with a very steep angle was identified on the northern shore of the island. Then a lineament with NE–SW trend, crossing the city of Ambon was observed. Last, a suspected quaternary normal fault was observed on the southern side of Ambon Bay.

Ambon and its surrounding islands (Seram, Haruku, Saparua, Nusa Laut, and Buru) have experienced at least 14 tsunamis in the historical past (Table 1). There were two events each generated by volcano activities and landslides, earthquakes (seven events), and three events with an undetermined source. The majority of the events are categorised to be minor tsunamis with a maximum height up to 2 m, except for the 1674 and 1899 events. The 1674 tsunami event was started by strong ground motion felt on Ambon Island. An extreme tsunami run-up up to 100 m was observed only on the southern shore of the island with minor tsunamis in other areas (Rumphius 1675). The source of this tsunami will be discussed in the following sections. In the 1899 event, settlements on Seram Island were devastated by an earthquake that was suspected of originating from the Kawa Fault (Soloviev and Go 1974). It triggered multiple landslides which generated tsunamis along the northern shore of Seram Island. The tsunami rose up to 9 m at villages of Amahai, Paulohi, and Elpaputih, with no reports of tsunami on the north coast of Ambon.

3. *Historical Accounts of the Ambon Island 1674 Earthquake and Tsunami*

Historical accounts of the 17 February 1674 Ambon earthquake and tsunami were documented in the book "Waerachtigh Verhael Van de Schlickelijcke Aerdbebinge" written by Rumphius (1675). The book was translated into English with the title "The true history of the terrible earthquake" (Rumphius 1997). The historical accounts described below are based on the English translation and summarised in Fig. 2 and Table 2.

The event occurred at about 7:30 p.m. local time when people in Laitimor were celebrating Chinese Lunar New Year. In Ambon, the bells in Victoria Castle swung by themselves and people who were standing fell to the ground as the earth heaved up and down like the sea. Stone buildings collapsed and buried up to 80 people. Strong shaking was felt on the mountains in Laitimor, with rocks falling and ground cracking open. In Hutumuri near the coast, on the eastern side of Laitimor, seawater burst into the air like a fountain.

The earthquake was reported from Hitu as well. In Waytome River, on the northern side, the river water spurted to 6 m high. People in the north to northwest of Hitu heard a loud sound like canon-fire. They noticed two long, thin marks in the sky, extending from Luhu to Seith, shortly before the earthquake. Less than 15 min after the earthquake, villages between Lima and Hila were wiped away by a gigantic mountain of seawater. The seawater rose about 50 to 60 fathoms (approximately 90–110 m) to the top of the surrounding hills, and more than 2300 people perished.

This unusual phenomenon was reported at other places, but with much less intensity. Hitu Lama village, located approximately 15 km to the east of Hila, reported that the seawater rose only about 3 to 5 m, killing 35 people. A little further to the east, 40 houses in Mamala were swept away without fatalities. The settlement of Orien (present name; Ureng), which is located < 10 km west of Lima reported that the seawater rose and inundated land but it did not enter the houses. People in Larike, a village in the westernmost of Hitu, observed that the seawater rose < 1 m at the Rotterdam Redoubt. In the southern and eastern areas of Ambon Island, there was much less seawater oscillation reported, apart from some small boats being tossed over each other.

At Luhu in Seram Kecil, the seawater inundated trees and the dwellings of a company. The water rose to a height just over 5 m. At the northernmost tip of Piru Bay, half of the houses in Tanuno were engulfed by water, but without fatalities. Fishermen in Piru Bay said the sea remained calm with a noticeable ripple. A much lower seawater oscillation was noticed by people from Manipa, Salati, Haruku, Nusa

Table 1

Historical tsunamis on Ambon and its surrounding islands between 1659 and 1950

Date	Source	Description	References
9–11 November 1659	Volcano: Mt Teon	A tsunami was noticed at Ambon Bay (1–1.5 m)	Wichmann (1918), Soloviev and Go (1974)
17 February 1674	Landslide triggered by an earthquake	Strong ground motion devastated Laitimor region followed by an extreme tsunami only on the northern shore of Hitu (100 m). A prolonged sequences of aftershocks was reported, with the largest occurring on 6 May generating a weak tsunami at Ambon Bay	Wichmann (1918), Soloviev and Go (1974), Rumphius (1675)
28 November 1708	Undetermined	A strong "tidal wave" suddenly burst into Ambon Bay and oscillated throught the night until the following morning. An earthquake was felt a day before	Wichmann (1918), Soloviev and Go (1974)
5 September 1711	Earthquake	A strong earthquake was felt on Haruku, Saparua, Nusa Laut, and Banda Islands. At Paso Baguala, eastern shore of Ambon, seawater rose by 1.2 m and destroyed two houses	Wichmann (1918), Soloviev and Go (1974)
18 August 1754	Earthquake	Houses on Ambon were destroyed by an earthquake. It was followed by a tsunami observed at Hutumuri, Haruku, and Saparua	Wichmann (1918), Soloviev and Go (1974)
19 April 1775	Earthquake	In the morning, a strong ground motion felt at Ambon Bay made the seawater oscillate	Wichmann (1918), Soloviev and Go (1974)
25 August 1802	Earthquake	Seawater rose and damaged the coast of Ambon after a strong earthquake was felt on the island	Wichmann (1918), Soloviev and Go (1974)
16 December 1841	Earthquake	A moderate earthquake was felt on Ambon, Buru, and Amblau Islands that generated a tsunami. The tsunami rose up to 1.5 m in height and swept away houses at Ambon Bay and Amblau. The aftershocks were reported until 21 December	Wichmann (1918), Soloviev and Go (1974)
26 November 1852	Earthquake	The Banda Islands were devastated by strong ground motion that was felt on Ambon. A tsunami arrived 15 min later on the Banda Islands and was reported at Ambon Bay up to 2 m height	Wichmann (1918), Soloviev and Go (1974)
10 June 1891	Undertermined	In the evening, seawater at Saparua Bay retreated about 200 m and then rapidly returned, inundating the shore. An earthquake was felt a day before	Soloviev and Go (1974)
7 June 1892	Volcano: Mt Awu	Eruption of Awu Volcano. A tsunami was noticed at Ambon Bay (1.5 m)	Soloviev and Go (1974)
30 September 1899	Landslide triggered by an earthquake	A strong earthquake was suspected as originating from the Kawa Fault devastated the settlements of Seram Island. It generated a tsunami that swept away villages at Elpaputih and Taluti Bays on the southern shore of Seram up to 9 m height. The tsunami was reported in a village on the eastern shore of Piru Bay as well, and noticed on Ambon	Soloviev and Go (1974)
5 July 1904	Undertermined	In the morning, seawater suddenly retreated and then rapidly returned, inundating the shore. An earthquake was felt a day before	Soloviev and Go (1974)
8 October 1950	Earthquake	An M 7.3 earthquake at south of Ambon generated a tsunami that arrived about 15 min later at Ambon Bay	Latief et al. (2016)

Table 2

Tsunami and ground motion interpretation from Rumphius (1997)

Location (region: village)	Description	Estimated tsunami height (m)	Estimated earthquake intensity
Hitu: Larike, Rotterdam Redoubt	Seawater rose to 2 feet high around the redoubt. The water rose three times without causing major damage other than crashing a boat	< 1 (inundation depth)	Undetermined
Hitu: Nusa Telo	Seawater rose suddenly after first withdrawing in the direction of Orien. The water oscillated three times from two directions		Undetermined
Hitu: Orien	A loud roar was heard in the air. The seawater rose then was drawn in the direction of Nusa Telo. The water did not enter houses but only surrounded the barricades		Undetermined
Hitu: Lima, Haarlem Redoubt	Seawater came from the direction of Lebalehu and rose about 50 or 60 fathoms around the redoubt, carrying stones, mud, and sand. Large boulders were thrown on the first floor of the redoubt. A woman was swept away 20 fathoms behind the redoubt. Lime kilns were washed away, with at least 86 fatalities	90–110 (run-up height)	Undetermined
Hitu: Seith	Seawater rose about 50 to 60 fathoms, up to the windows of the fort. Villages between Seith, Lebalehu, and Wasela were washed away (but Hautunua village at a higher location was safe). Lime kilns were washed away, with more than 619 fatalities	90–110 (run-up height)	Strong
Hitu: Lebalehu	A 200 m-wide region around Lebalehu collapsed, making the beach very steep. This also happened between Seith and Hila (west of Fort Amsterdam), including Nukunali, Taela, and Wawani. An upwelling of seawater (to about 50 or 60 fathoms) originated from here, dividing into three: (i) east—Seith and Hila, (ii) west—Lima and Orien, (iii) to the sea. The water glowed like fire but was as black as coal and noisy. Lime kilns were destroyed	90–110 (run-up height)	Strong
Hitu: Hila, Fort Amsterdam	At least 1461 people were killed. Seawater rose between 50 and 60 fathoms high to the gallery of the fort and overtopped the roof. All the houses around the fort were swept away, particularly to the west and south. A grinding wheel, a drum, a large coral, fish cages, and cattle were swept away	90–110 (run-up height)	Strong
Hitu: Hitu Lama	Seawater rose 10 feet and swept away several houses. About 35 people were killed	3–5 (inundation depth)	Undetermined
Hitu: Mamala and Waytome River	40 houses were swept away, without fatalities. Limekilns were destroyed. Strong ground motion toppled equipment inside a warehouse. Eastern shore of Waytome River split open and water spurted 18–20 feet high	< 2 m (inundation depth)	Felt (Mamala)–Strong (Waytome River)
Hitu: Liang	The earthquake was felt with no damage to the houses		Felt
Hitu: Way	The earthquake was felt with no damage to the houses		Felt
Hitu: Tulehu	The earthquake was felt with no damage to the houses		Felt
Hitu: Thiel	A few houses were carried away by seawater		Undetermined
Laitimor: Paso Baguala, Fort Middleburg	Weapons and equipment were damaged. The earth around Baguala and Hutumuri cracked. Seawater came from the direction of Fort Victoria but did not overflow the isthmus		Strong
Laitimor: Hutumuri, near to the shore	Seawater burst upwards like a fountain		Strong
Laitimor: Cape Nusanive	Boats were tipped over and fishermen noticed the waves were a little higher than normal		Undetermined
Laitimor: Ambon, Victoria Castle	Bells in the castle swung by themselves. People around the castle fell over and saw the ground heaving up and down like the sea. Central walls of the town hall collapsed. A hospital was badly damaged. Boats at the mouth of Oliphant River were thrown into the stream. The bridge close by was almost shaken loose. Goods in houses shifted 3 to 4 feet without breaking. 79 people were killed and more than 35 injured when at least 75 buildings collapsed		Strong
Seram Kecil: Cape Sial	Seawater caused damaged		Undetermined

Table 2 *continued*

Location (region: village)	Description	Estimated tsunami height (m)	Estimated earthquake intensity
Seram Kecil: Luhu, Overburg Redoubt	Villages and boats were swept away. Seawater rose 3 fathoms above normal	5.5	Undetermined
Seram Kecil: Tanuno	Seawater rose once and half the houses were swept away, without fatalities. Fishermen claimed that the sea in Piru Bay was calm		Undetermined
Haruku: Oma	Earthquake described as violent, small rocks fell into the sea and a large boulder was moved. Seawater rose 6 feet above normal	2	Strong
Nusa Laut	Earthquake described as violent		Strong
Banda Islands: Neira	Earthquake described as moderate. Seawater rose a little, but no damage		Moderate
Buru	Earthquake was felt		Felt
Amblau	Earthquake was felt		Felt
Manipa	Earthquake was felt. Seawater rose at Fort Manipa. 40 houses swept away, but no fatalities	1–2	Felt
Kelang: Salati	Earthquake was felt. Seawater rose 6 feet above normal	2	Felt
Boano	Earthquake was felt		Felt
Laitimor: Nacau	Strong earthquake made seven houses collapse, large rocks fell		Strong
Laitimor: Ema -Soya	Road was cracked 2 to 3 feet wide in several places		Strong

Laut, and Banda Neira Island compared with the oscillation that was observed in Hitu and Laitimor. Aftershocks continued for at least 3 months. The two largest aftershocks occurred on 6 and 10 May.

What were the source of the ground motion and seawater phenomena described above, particularly on 17 February 1674? In the following sections, we will make use of the historical accounts of ground motion and tsunami observation to answer that question.

4. Source Identification

4.1. Earthquake Source

With regard to the tectonic setting around Ambon, there are five candidate faults that could have generated a large earthquake with the intensities and effects shown in Fig. 2: (1) the north Seram Megathrust, (2) the Kawa Fault, (3) an intraslab fault (4) the purported South Seram Thrust Fault, or (5) a local fault on Ambon. Each of these is qualitatively analysed below to identify the most credible source of this event.

In general, the strongest ground motions were felt on Laitimor, Oma (Haruku), and Nusa Laut (Fig. 2). The intensity of ground motion decreases toward Banda Neira in the south, and Boano in the north. Many buildings collapsed and ground cracked in various places on Laitimor. There was liquefaction at Hutumuri and Waytome Rivers according to the accounts of *'water spurt[ing] high [in]to the air'*. Recurring aftershocks were reported until at least 10 May. Judging by these observations, the source must have been a moderate to large earthquake with a local and shallow epicentre.

A shallow earthquake on the north Seram Megathrust would have been too far from Ambon to have these effects and if the earthquake had occurred on this fault, the islands of Boano, Kelang, and Manipa where moderate shaking was reported (Fig. 2) should have experienced stronger ground shaking than Ambon and Banda Neira. If the earthquake had originated from the Kawa Fault, the villages on Seram Island would have experienced more intense ground shaking as in the 1899 earthquake and tsunami event (Soloviev and Go 1974). A deep intraslab earthquake would generate ground motion felt over a broader region. However, deep intraslab earthquakes typically do not cause ground cracking and long aftershock sequences. The Benioff zone is over 100 km beneath Ambon (Spakman and Hall 2010), and an intraslab earthquake at this depth would likely generate strong ground motion distributed over a wider area than observed.

Therefore, credible sources for this event could have be the South Seram Thrust Fault or a local fault

on Ambon. The South Seram Thrust was used in seismic and tsunami hazard maps of Indonesia (Irsyam et al. 2010; Horspool et al. 2014), where it is indicated as running from the south shore of Buru to Nusa Laut with northward dip (Fig. 1). Although there is apparently evidence for this fault in proprietary marine seismic survey results (J. Griffin, personal communication 2018), we note that it does not appear on the most recent revision of Indonesia's seismic hazard map (Irsyam et al. 2019). We therefore regard the existence of this fault as speculative, even though an earthquake on it could have caused the observed ground shaking. Brouwer (1921) and Watkinson and Hall (2017) have confidently identified quaternary faults on Ambon itself, one of which Harris and Major (2017) identified as the source of the 1674 earthquake without a clear explanation of why. We conclude that any of these faults on and near Ambon could have generated the observed ground shaking, but further investigation is required to determine exactly which one ruptured in 1674.

4.2. *Tsunami Source*

If we consider which of the five candidate faults previously mentioned might have been capable of directly generating the observed tsunami, it is immediately obvious that an intraslab event could not, since an earthquake deeper than 100 km in the Benioff zone beneath the Banda islands could generate only a weak tsunami at best. Okal and Reymond (2003) showed that the largest intraslab event ever recorded, the 1938 $M_w = 8.5$ Banda Sea event at 60 km depth, generated only a weak tsunami. A tsunami generated by the Seram Megathrust or South Seram Thrust would have to enter Piru Bay through narrow straits around Ambon Island, which would greatly attenuate the tsunami arriving on the north coast of Ambon. As we show in Sect. 6 below, instead of having highest run-up along the north coast of Ambon, the tsunami energy generated by these two scenarios would be concentrated between the western and southern coast of Hitu and Laitimor, respectively. The Kawa Fault has a strike-slip mechanism that might generate a significant local tsunami generation where it crosses the southern shore of Seram, such as occurred in the 1994 Mindoro (Imamura et al. 1995) and 2018 Palu (e.g. Jamelot et al. 2019) events. However, it seems unlikely this mechanism could generate high tsunami run-up only along the northern coast of Ambon.

The only fault that might generate a large tsunami on the northern coast of Ambon and nowhere else would be a local fault documented on the northern shore of Hitu (Brouwer 1921; Watkinson and Hall 2017). The fault has a normal mechanism that could generate vertical displacement of a water column for tsunami generation. However, the fault under consideration is only 16 km long, and therefore unlikely to generate an earthquake with magnitude < 7 and slip much higher than 2 m (Kanamori and Anderson 1975; Geller 1976; Wells and Coppersmith 1994), far too small to generate the observed tsunami run-up. Therefore, if none of the potential tsunamigenic earthquakes could have been capable of directly generating a tsunami with the observed run-up, the most plausible source of the tsunami is from an earthquake-triggered landslide in Piru Bay.

There is an indication in Rumphius' accounts 1997 that a massive coastal landslide occurred on the northern shore of Hitu, between Seith and Hila.

> The country around Lebalehu, a region once famed for its market and for being the most important Muslim meeting place, collapsed the width of a Musquet shot. There is no longer any beach there, but only a very steep precipice. Just the same is true between Ceyt (Seith) and Hila, even as far as the beach at the later place, along the west side of the Fort Amsterdam and beneath the Residence of Intche Tay. Including the Negeris Nukunali, Taela and Wawani, all this disappeared along with [the] roadstead where ships used to anchor. It seems likely that the aforementioned wall of water arose in the place just indicated, to wit directly below Lebalehu. It might even have come from Hitu because various people on board ships that were not far off shore, reported only a rippling of the waves. The mass of upwelling water divided into three parts. One went east to Ceyt (Seith) and Hila, the other west to the villages of Lima and Oried. The water stank so horribly that people on board ships close to the coast became ill, and it was so filthy that anyone who

had been immersed in it looked as if he had been hauled out of a mudbath.

In other words, there was a major change in the landscape around the coastal region: a gentle beach became very steep. Moreover, people saw that the water was dark and a roaring sound was heard from this area, which indicates that the seawater mixed with sediment and the tsunami source was near the people. The seawater colour and loud sound described in the accounts are similar to those described after the 1998 Aitape, Papua New Guinea (PNG) tsunami (Davies et al. 2003), which is thought to have been generated by a landslide. Unfortunately, there is no further information with regard to parameters of the landslide. According to the accounts, it was a partially subaerial landslide, with about 200 m of the previous shoreline collapsing into the sea. The lateral extent is thought to be at least 5 km along the coastline between the villages of Seith and Hila.

Further, the majority of the fatalities in this event were in this region and not many buildings collapsed in the earthquake. In addition, an extreme run-up laterally along the coastline can only be explained by a landslide. These observations are similar to the 1998 Aitape, PNG tsunami, which was generated by an underwater landslide (Okal and Synolakis 2004; Synolakis et al. 2002).

5. *Landslide-Generating Tsunami*

Tsunami generation is affected by both the vertical and length extent of the displace bathymetry (Heidarzadeh et al. 2014). Vertical displacement due to an earthquake normally reaches only a few metres at most, whereas it can easily reach hundreds of metres in a mass failure event. The dimensions of an earthquake rupture can extend to hundreds of kilometres but it is rare to see a huge landslide up to 100 km length. Therefore, a tsunami generated by an earthquake has a long wavelength as it travels across the ocean. On the other hand, a tsunami generated by a landslide loses its energy quickly as it travels because of its shorter wavelength, but it has a much larger amplitude in a local area. Therefore, tsunamis generated by earthquakes can be observed over a wide area, with a relatively constant run-up along the coastline. In contrast, a narrow region of extreme run-up is observed in a tsunami event generated by a landslide.

Okal and Synolakis (2004) investigated tsunami height profiles along a coastline from some past tsunami events. They found similar patterns in the 1946 Unimak (Alaska) and 1998 Aitape (PNG) tsunami profiles, which were both generated by landslides. The profiles had extreme run-up heights over a very narrow along-shore extent. Based on these findings, Okal and Synolakis (2004) developed a criterion for identifying landslide-generated tsunami based on the aspect ratio $I_2 = \frac{b}{a}$ between the maximum tsunami run-up height b and the distance a of the lateral extent of high tsunami run-up along the coastline. Thus, any event with I_2 larger than 0.0001 should be considered a tsunami generated by a landslide.

Accordingly, we calculate the I_2 of the tsunami observations on the northern coast of Hitu. It was difficult to determine the exact values of a and b because of the sparse data available (Fig. 3a). However, the data clearly shows a very rapid drop in run-up to the east and west of the maximum run-up height location between Lima and Hila. The estimated I_2 was > 0.006, which was 60 times larger than the limit suggested by Okal and Synolakis (2004). Therefore, this tsunami almost certainly was generated by a landslide.

6. *Tsunami Modelling*

Tsunami modelling was performed to confirm the analysis above using the JAGURS tsunami simulation code (Baba et al. 2015, 2017). The code numerically solves the shallow water wave equations in a spherical coordinate system with a finite-difference scheme. The digital elevation model (DEM) was built from a combination of nautical charts, a 90-m commercial bathymetry dataset provided by the TCarta Marine, the General Bathymetric Chart of the Oceans (GEBCO), and the SRTM-90m in a domain of nested grids (Fig. 4). The coarsest and finest grid resolution of the domain is approximately 1500 and

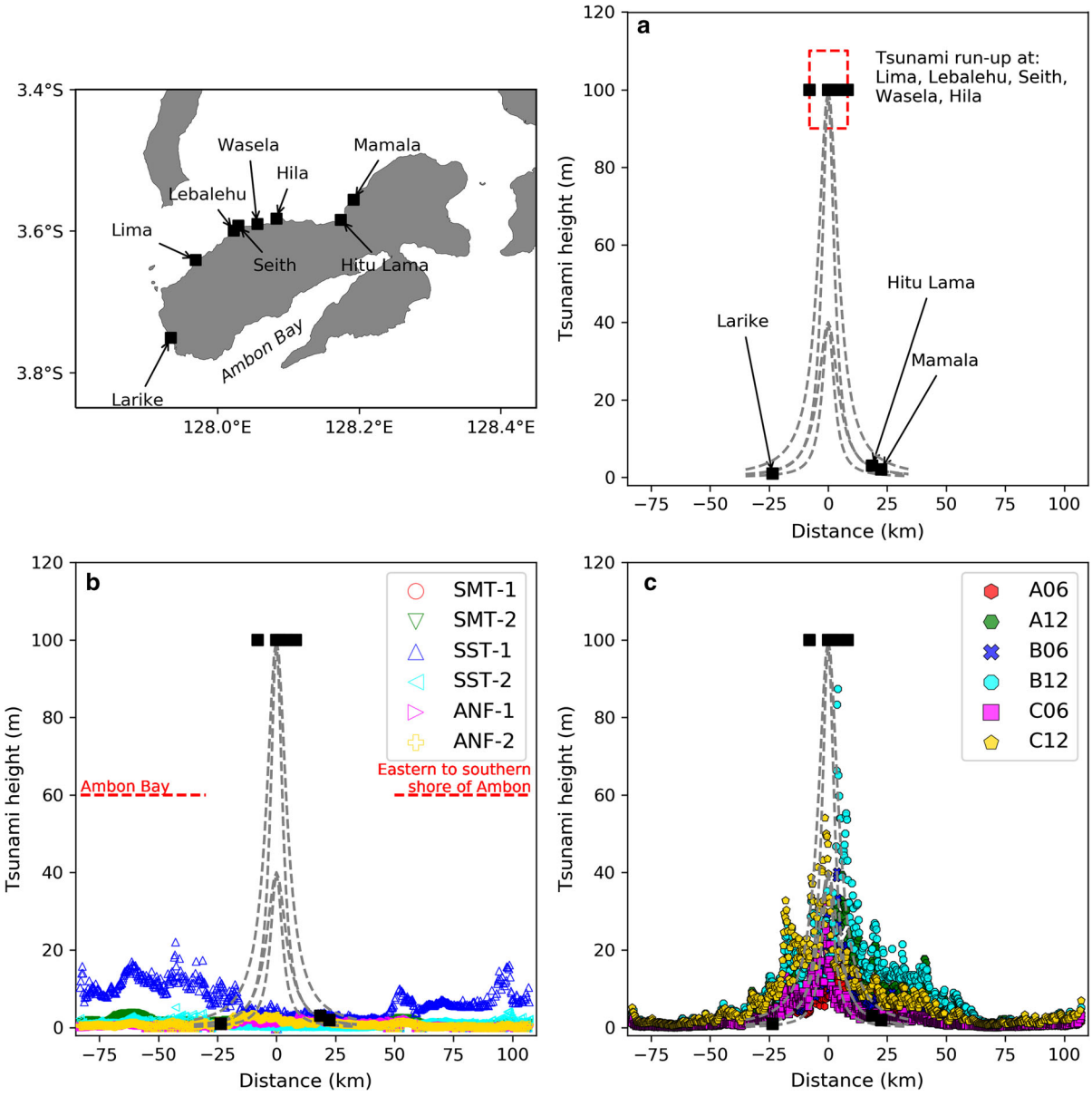

Figure 3
Tsunami height profiles along the coastline: **a** black squares are data; the dashed lines indicate I_2 of $a = 3$–5 km with $b = 40$–100 m; **b** only from tsunamigenic earthquake scenarios; **c** selected landslide-generating tsunami scenarios. Symbols with colour indicate the scenario codes as shown in Tables 3 and 4

167 m, respectively. A time-step of 0.5 s is set to satisfy the Currant stability condition.

Tsunami simulations were conducted for tsunamigenic earthquake (Table 3) and landslide-generated tsunami scenarios in this area (Table 4). The initial sea surface elevation from the earthquake scenarios were assumed to be equal to the earthquake deformation calculated from the Okada (1985) formula, using the parameters discussed below.

A two-layer model was utilised to simulate tsunami generation and propagation due to a landslide (Baba et al. 2019). As with the single-layer, earthquake-generated tsunami simulation, the two-layer simulation requires specification of ocean depth (i.e.,

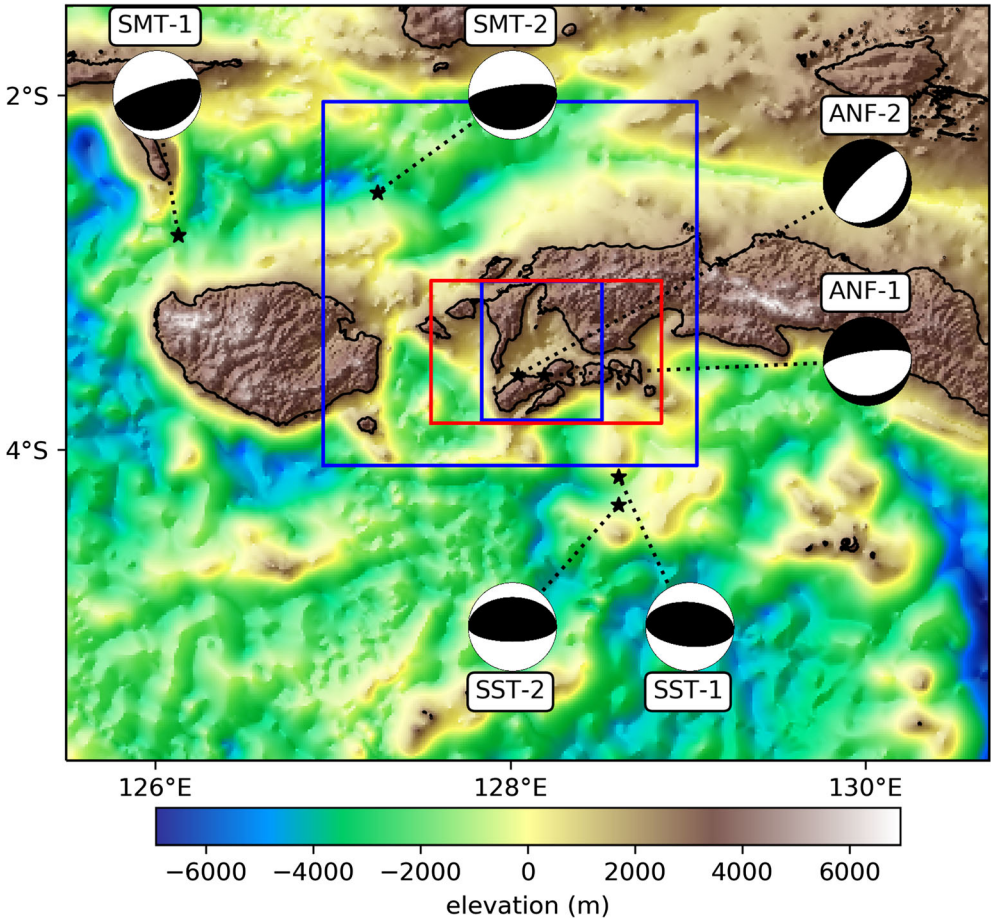

Figure 4
Domain model of tsunami modelling. The blue boxes are the nested-grids domain for the tsunamigenic earthquake model and red box shows the domain model for landslide-generating tsunami scenarios. Beach balls and black starts represent scenarios on Table 3

bathymetry). In addition, the two-layer simulation requires an initial condition for the depth to the top of a viscous fluid layer, which is allowed to flow in response to gravity, exciting a tsunami by displacing the ocean layer above it (see Baba et al. (2019) for further details of the two-layer algorithm). The two-layer simulation was performed in a single grid domain model, over a tsunami propagation time of 2 h with time-step of 0.25 s.

6.1. Tsunamigenic Earthquake Scenarios

SMT-1 and SMT-2 (Fig. 5) represent two earthquake scenarios from the Seram Megathrust zone. The M_w = 8.2 parameters of SMT-1 (Løvholt et al. 2012) were speculated to be the source of the events documented in 1657, 1708, 1876, and 1965 (note that here and in subsequent sections, we use M_w to denote an input parameter for tsunami modelling, not a magnitude estimated for a historical earthquake). According to Horspool et al. (2014) and Irsyam et al. (2010), the Seram Megathrust zone is capable of generating an earthquake with a maximum $M_w = 7.9$ to 8.2. Here, SMT-2 represents an earthquake with $M_w = 8.1$ with the fault parameters taken from Horspool et al. (2014).

SST-1 and SST-2 (Fig. 5) represent two scenarios from the South Seram Thrust Fault. Løvholt et al. (2012) assumed the 1674 Ambon tsunami was caused by an $M_w = 8.1$ earthquake on the South Seram Thrust Fault. The authors suggested that the same fault zone triggered the 1950 and 1983 events. The source parameters of the SST-1 scenario were taken from

Table 3

Tsunamigenic earthquake scenarios for the 1674 Ambon event

Scenario	Position[a]	Length (km)	Width (km)	Strike	Dip	Rake	Slip (m)	Mo (Nm)
2.2SMT-1	2.97° S, 126.13° E, 0 km	202	80	73°	20°	90°	8.0	2.24×10^{21}
SMT-2	2.55° S, 127.25° E, 5 km	180	90	83°	20°	90°	5.0	1.58×10^{21}
SST-1	4.15° S, 128.61° E, 0 km	179	80	− 85°	40°	90°	7.0	1.58×10^{21}
SST-2	4.31° S, 128.61° E, 5 km	70	40	− 90°	30°	90°	1.5	2.00×10^{20}
ANF-1	3.58° S, 128.19° E, 2 km	25	10	− 98°	70°	− 90°	5.0	1.12×10^{18}
ANF-2	3.58° S, 128.04° E, 2 km	20	10	− 135°	70°	− 90°	5.0	6.31×10^{18}

Position[a]: top-right corner coordinate of a fault plane

Table 4

Landslide-generating tsunami scenarios

Centre of the Gaussian		
Location	Longitude	Latitude
A	128.07° E	3.585° S
B	128.03° E	3.585° S
C	128.02° E	3.585° S
Gaussian parameters		
ID	Radius (m)	Thickness (m)
1	500	100
2	500	200
3	500	300
4	1000	100
5	1000	200
6	1000	300
7	2000	100
8	2000	200
9	2000	300
10	2500	100
11	2500	200
12	2500	300

their study. Another study conducted by Latief et al. (2016) indicated the source of the 1950 Ambon tsunami as being on the South Seram Thrust Fault, but it was located a little further south, with a smaller fault plane. The SST-2 scenario followed the parameters used in Latief et al. (2016) and is represented as an $M_w = 7.5$ earthquake.

Finally, ANF-1 and ANF-2 (Fig. 5) were designed to follow the normal fault, as indicated by Brouwer (1921) and Watkinson and Hall (2017), respectively. These two scenarios represent earthquakes with $M_w = 6.0$ to 6.5, respectively. They are only hypothetical scenarios because no detailed study has been conducted on these faults, other than categorisation as quaternary faults (Watkinson and Hall 2017). Here a dip of 70° was selected as the optimum angle of a normal fault earthquake to generate maximum vertical displacement.

6.2. Landslide-Generating Tsunami Scenarios

We tested 36 synthetic scenarios of landslide-generating tsunami models (Table 4). The landslide layer was assumed to have a Gaussian function on top of the recent DEM with a deformable material type. The radius and thickness of the Gaussian varied from 500 to 2500 m and between 100 and 300 m, respectively. It was located at three different places (A, B, C) near the shoreline between Seith and Hila. The locations were selected according to the accounts previously discussed. To satisfy the stability of the model, the landslide layer needed to be 'clipped', so that the landslide would always remain below the at-rest level of the sea surface. Therefore, the landslide layer looked like a Gaussian-shaped accumulation of sediment that is clipped where it emerges above the water surface (Fig. 6).

7. Results and Discussion

Piru Bay is a nearly closed sea surrounded by several narrow straits surrounding Ambon Island. It is difficult for much tsunami energy to propagate from outside the bay to Ambon's northern shore, particularly in the SMT-1, SMT-2, SST-1, and SST-2

Figure 5

Initial sea surface elevation from tsunamigenic earthquake scenarios shown in Table 3. SMT-1 and SMT-2 represent the Seram Megathrust; SST-1 and SST-2 are the South Serahm Thrust; and ANF-1 and ANF-2 are local faults on the Ambon scenarios. Each figure has a different colour scale

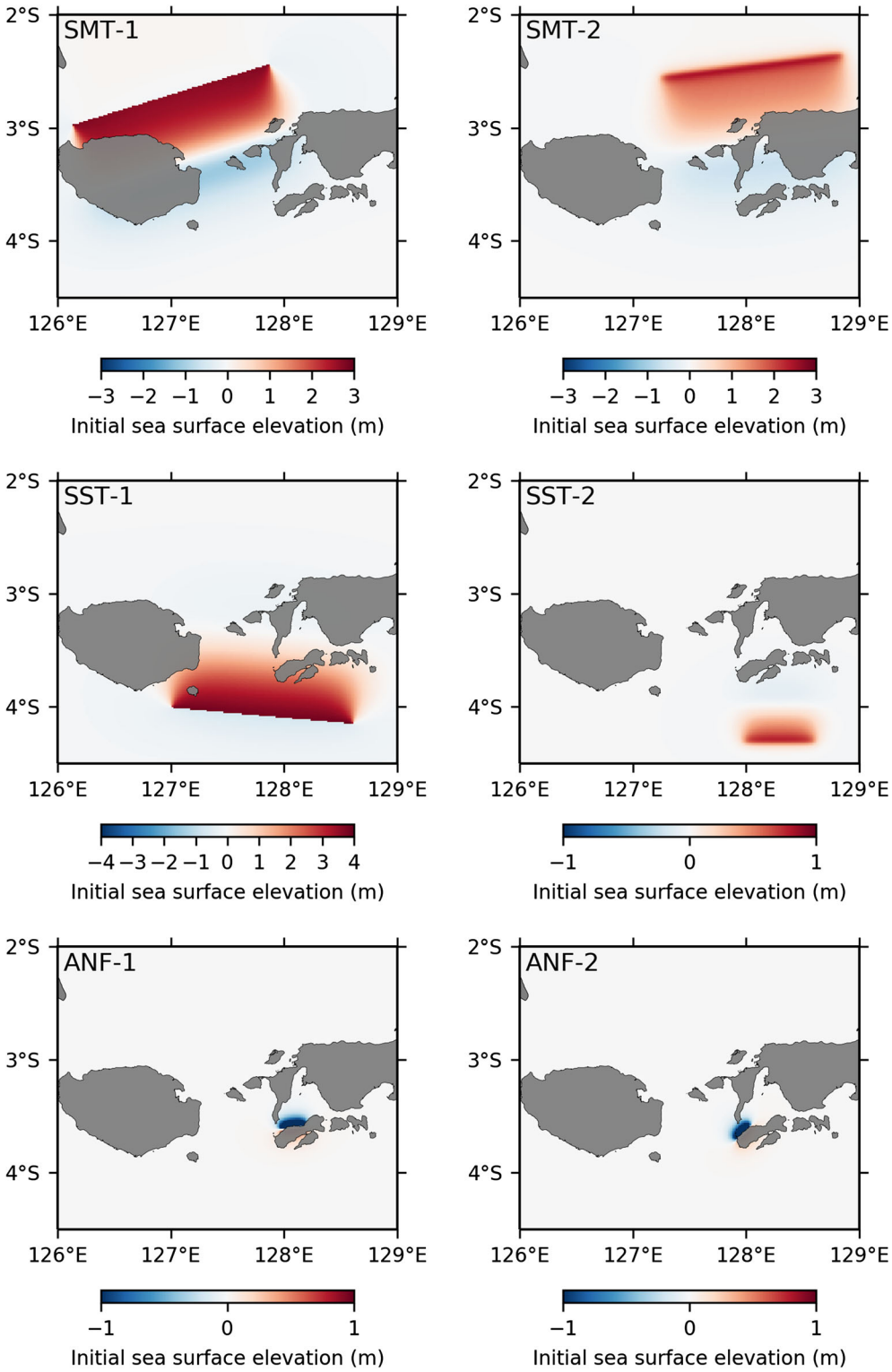
SMT-1
SMT-2
SST-1
SST-2
ANF-1
ANF-2
2°S
3°S
4°S
126°E
127°E
128°E
129°E
−3 −2 −1 0 1 2 3
−4 −3 −2 −1 0 1 2 3 4
−1 0 1
Initial sea surface elevation (m)

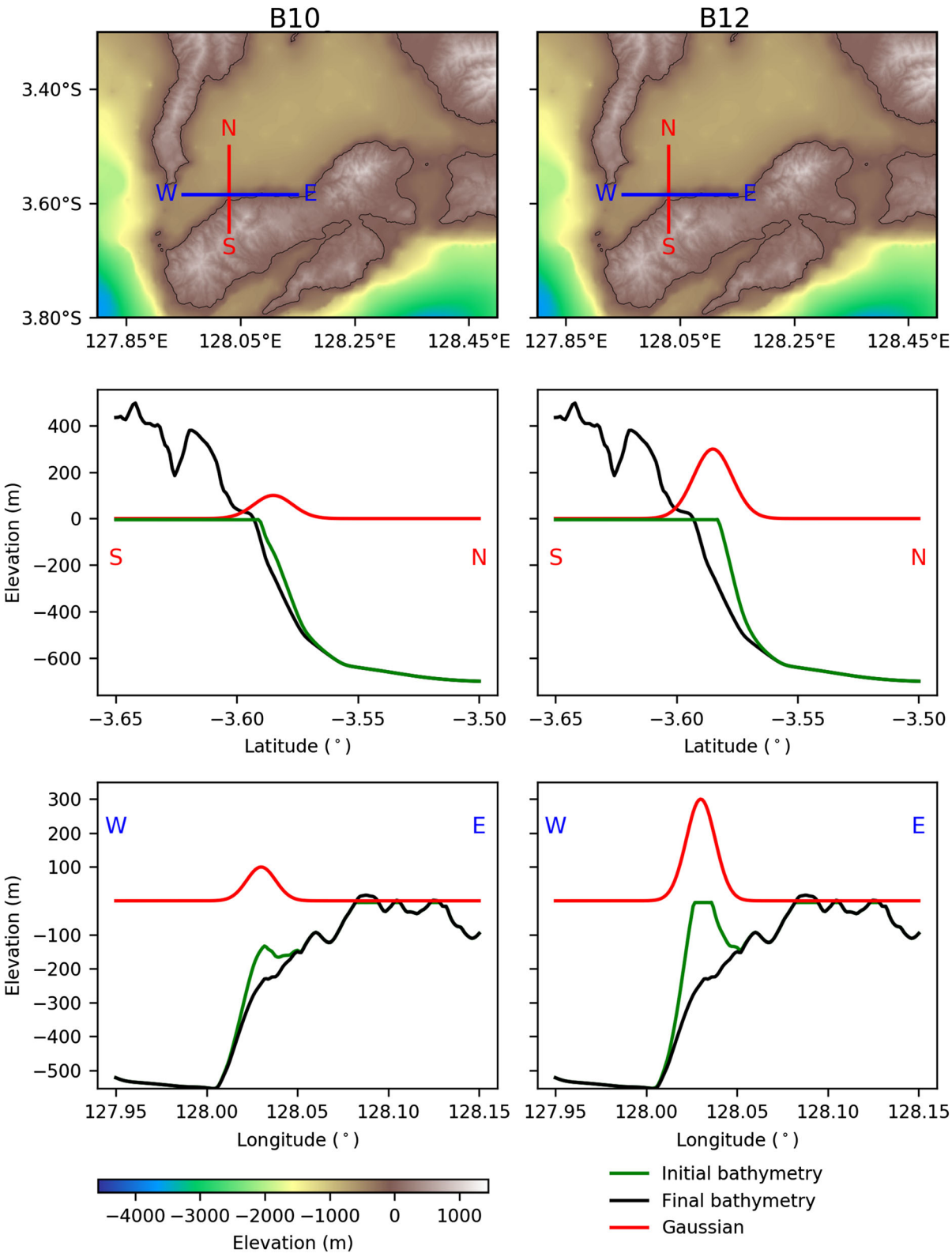
B10
B12
3.40°S
3.60°S
3.80°S
127.85°E
128.05°E
128.25°E
128.45°E
N
W
E
S
Elevation (m)
Latitude (°)
Longitude (°)
−3.65
−3.60
−3.55
−3.50
127.95
128.00
128.05
128.10
128.15
−4000 −3000 −2000 −1000 0 1000
Elevation (m)
Initial bathymetry
Final bathymetry
Gaussian

◀Figure 6
Illustration of selected tsunami landslide scenarios shown in Table 4. B10 and B12 are landslides with the centre of the Gaussian located at Point B (128.030° E and 3.583° S) with each radius of 2500 m and maximum thickness of 100 and 300 m, respectively. The middle and bottom figures are 'clipped' initial bathymetry (green), final bathymetry (black), and the Gaussian (red) profiles along the W–E and N–S direction

scenarios. Therefore, the maximum tsunami amplitude simulated was relatively small (Fig. 7). These results meant that a tsunami source inside the bay is required.

As suspected, no tsunamigenic earthquake model could generate a high tsunami inside Piru Bay only, with the maximum height located on the northern shore of Ambon, except the normal fault scenarios (Fig. 3b). However, the fault length limits the magnitude, requiring a huge slip to produce a very high tsunami. This would be an unrealistic model. The normal fault model scenarios in this study were already unrealistic, with a 5-m slip.

All the landslide-generating tsunami simulations result in a maximum tsunami height concentrated inside Piru Bay between Seith and Hila with minor tsunamis at the other places (Fig. 8). Through these simulations, we confirm the tsunami height distribution mentioned in the historical accounts (Rumphius 1675). The largest tsunami height near the shoreline is almost 80 m from the B12[1] landslide scenario, with an approximate volume of 1 km^3 (Fig. 3c).

The 100 m tsunami run-up between Seith and Hila villages could not be reconstructed for several reasons. First, there was no high-resolution DEM available to accommodate detailed inundation modelling. Therefore, the tsunami height profiles were extracted along the depth of 20 m and Green's law (Synolakis 1991) was used to estimate the run-up height on the shoreline. Second, any DEM would not represent the actual elevation at that time. Third, it was possible that the tsunami run-up reported had been exaggerated. For example, *'the water rose especially between those villages (Lima and Hila) and Seith to the top of the surrounding hills, estimated to be some 50 to 60 fathoms [90–110 m] high'*. This account could have meant a maximum run-up height due to water splash. According to the recent DEM, the closest hill with a height above 100 m was located about 500 to 1500 m from the shoreline, meaning the northern coast had a narrow backed strip coastal by steep topography. Moreover, some accounts noted seawater rising as high as the window of a redoubt in Seith and over-topping Fort Amsterdam in Hila. According to the online photos available, all the redoubts and forts are located near the coastline and are two to three floors high (approximately 20–30 m). Therefore, our simulated landslide scenario produced a reasonable tsunami height.

Although the primary source of the ground motion was still unclear, it was most likely from a local and shallow earthquake. From the reports of ground cracking and building damage in Laitimor region, the earthquake location was most likely south of Ambon or Nusa Laut, with the northern limit in the Laitimor region. Further investigation is highly recommended.

7.1. Limitations

Because our DEM cannot resolve evidence of a slump, confirmation of this finding through a high-resolution bathymetric survey, as well as a more sophisticated landslide-generating tsunami model is needed. The two-layer model in the JAGURS code considered only a submarine landslide type. Therefore, as noted earlier, the landslide layer had to be 'clipped' to keep it below sea level, for code stability, which may have resulted in underestimating the actual condition. In addition, the code was a frictionless model, so the slide layer did not stop moving during the simulation.

7.2. Implications for the Other Historical Accounts

The primary source of this earthquake and tsunami was confirmed from the sparse historical accounts (Rumphius 1997). While the precise mechanism of the earthquake remains unclear, the source of the tsunami could be confirmed to be a coastal landslide.

This study has shown a technique for optimising sparse and incomplete accounts. The historical accounts of tsunamis in Indonesia have been documented in several catalogues (e.g. Wichmann

[1] A landslide located at Point B from ID-12—Table 4.

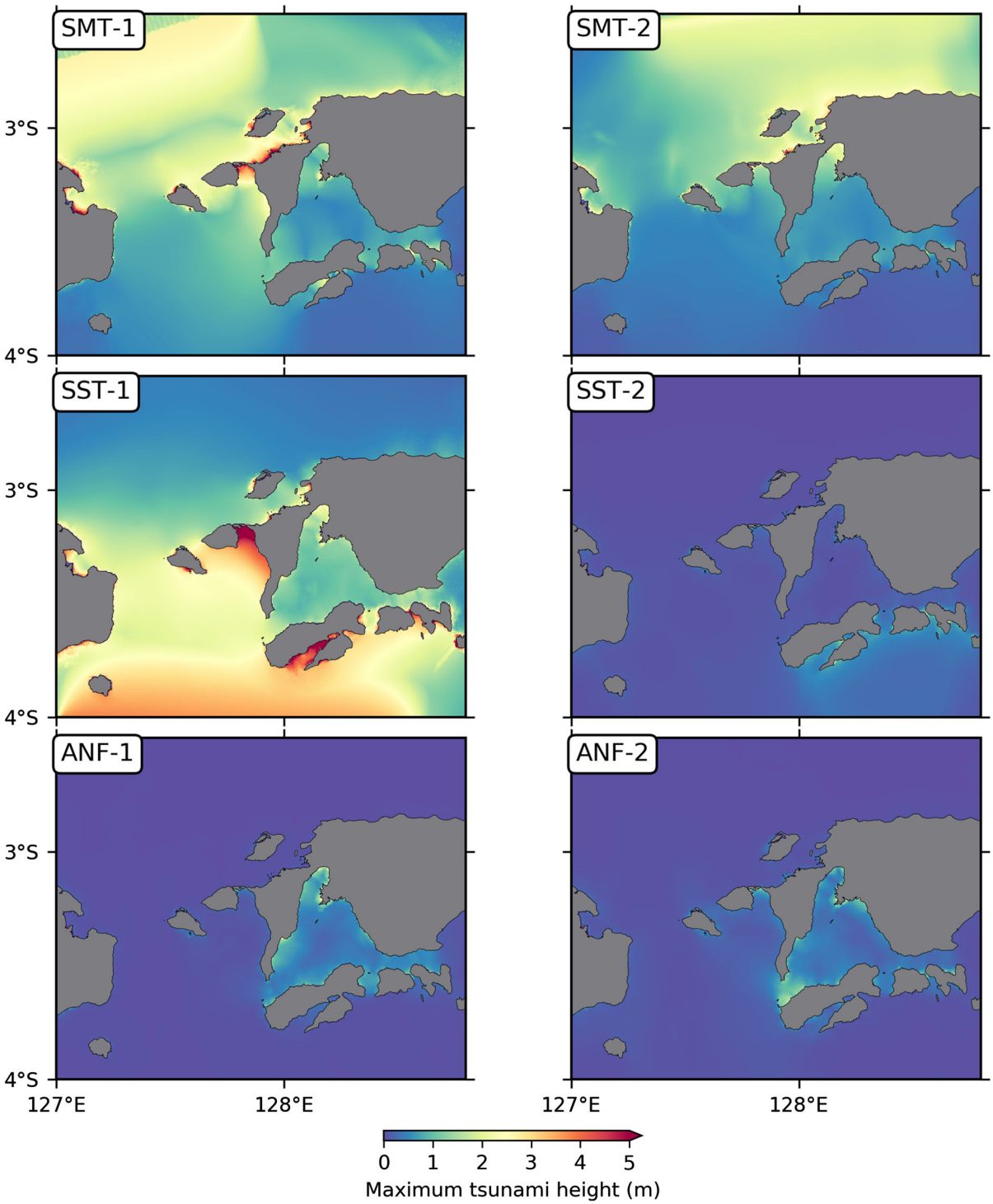

Figure 7
Maximum tsunami heights from the tsunamigenic earthquake scenarios shown in Fig. 5

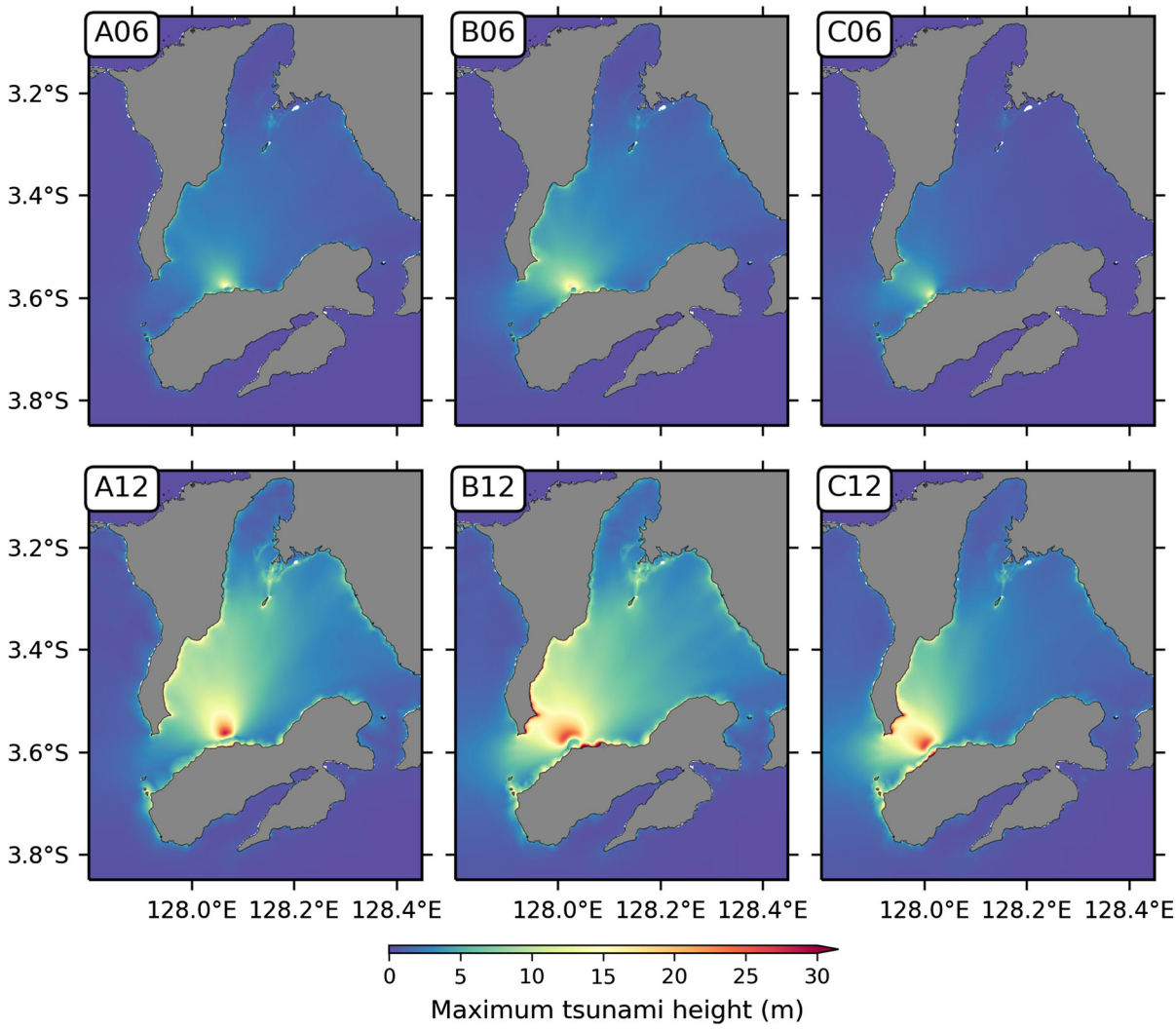

Figure 8
Selected maximum tsunami height from landslide scenarios shown in Table 4

1918, 1922; Soloviev and Go 1974; Soloviev et al. 1986). Generally, all accounts of tsunami events began by describing ground motion felt at various places with different intensities. These were followed by tsunami heights observation along the coastline. For the 1674 Ambon event, there is no detailed information regarding the source of the ground motion, nor the tsunami. By using similar technique that used in this study, the primary source of the tsunamis noted in the catalogue might be changed and/or updated in more detail. For example, the primary source of the devastating 1899 Seram tsunami was associated with an earthquake from the Kawa Fault. The kind of analysis we have employed here might help resolve whether the tsunami was generated by coseismic displacement where the strike-slip fault crosses the shore, such as occurred in the 1994 Mindoro (Imamura et al. 1995) and the 2018 Palu (Jamelot et al. 2019) events, or was mainly caused by the landslides observed along the southern coast of Seram (Soloviev and Go 1974).

Investigating other historical accounts will help to reveal more about the most likely primary source of the tsunami in each region. This will allow a more comprehensive tsunami hazard assessment.

8. Conclusion

In this study we have shown how historical accounts of the 1674 Ambon tsunami, one of Indonesia's largest and deadliest tsunami disasters, can be used to better understand its earthquake source and mechanism of generation. We have shown that, although the reports of ground motion intensity and damage fail to definitively identify the earthquake source, it is almost certain that it was local and shallow, probably either a crustal fault on Ambon itself or the putative South Seram Thrust Fault off its southern coast.

More significantly, we have shown that the only way to explain the extreme run-up only on the northern shore of Ambon, and in particular the very narrow lateral extent along the coast over which it occurred, is by attributing the tsunami generation to a submarine landslide. Tsunami scenario simulations showed that plausible earthquake sources could not generate such a run-up profile, but a submarine landslide of about 1 km^3 volume, consistent with eyewitness accounts of dramatic changes in the coastal landscape, could produce run-up commensurate with the historical observations.

Our analysis of the 1674 Ambon tsunami suggests that, as suggested by more recent events like the 1992 Flores and 2018 Palu and Sunda Straight tsunamis (Pranantyo and Cummins 2019; Sassa and Takagawa 2019; Giachetti et al. 2012; Patton et al. 2018, respectively), submarine landslides are an important component of the tsunami threat in Indonesia and should be considered in future tsunami hazard assessments. We believe further work on this and other historical events, especially when combined with paleotsunami and bathymetric surveys, can provide important constraints on the unique nature of the tsunami threat in regions of particularly complex and active tectonics like eastern Indonesia.

References

Audley-Charles, M., Carter, D., Barber, A., Norvick, M., & Tjokrosapoetro, S. (1979). Reinterpretation of the geology of Seram: Implications for the Banda Arcs and northern Australia. *Journal of the Geological Society*, *136*(5), 547–566.

Baba, T., Allgeyer, S., Hossen, J., Cummins, P. R., Tsushima, H., Imai, K., et al. (2017). Accurate numerical simulation of the far-field tsunami caused by the 2011 Tohoku earthquake, including the effects of Boussinesq dispersion, seawater density stratification, elastic loading, and gravitational potential change. *Ocean Modelling*, *111*, 46–54. https://doi.org/10.1016/j.ocemod.2017.01.002.

Baba, T., Gon, Y., Imai, K., Yamashita, K., Matsuno, T., Hayashi, M., & Ichihara, H. (2019). Modelling of a dispersive tsunami caused by a submarine landslide based on detailed bathymetry of the continental slope in Japan Nankai trough, southwest Japan. *Tectonophysics*, *768* (228182). https://doi.org/10.1016/j.tecto.2019.228182.

Baba, T., Takahashi, N., Kaneda, Y., Ando, K., Matsuoka, D., & Kato, T. (2015). Parallel implementation of dispersive tsunami wave modeling with a nesting algorithm for the 2011 Tohoku tsunami. *Pure and Applied Geophysics*, *172*(12), 3455–3472. https://doi.org/10.1007/s00024-015-1049-2.

Brouwer, H. (1921). Some relations of earthquakes to geologic structure in the East Indian Archipelago. *Bulletin of the Seismological Society of America*, *11*(3–4), 166–182.

Davies, H., Davies, J., Perembo, R., & Lus, W. (2003). The Aitape 1998 tsunami: Reconstructing the event from interviews and field mapping. In J. P. Bardet, F. Imamura, C. E. Synolakis, E. A. Okal, & H. L. Davies (Eds.), *Landslide tsunamis: Recent findings and research directions* (pp. 1895–1922). Basel: Springer. https://doi.org/10.1007/978-3-0348-7995-8_7.

Geller, R. J. (1976). Scaling relations for earthquake source parameters and magnitudes. *Bulletin of the Seismological Society of America*, *66*(5), 1501–1523.

Giachetti, T., Paris, R., Kelfoun, K., & Ontowirjo, B. (2012). Tsunami hazard related to a flank collapse of Anak Krakatau volcano, Sunda Strait, Indonesia. *Geological Society, London, Special Publications*, *361*(1), 79–90. https://doi.org/10.1144/SP361.7.

Hamilton, W. (1979). *Tectonics of the Indonesian region* (4th ed.). Washington: United States Government Printing Office.

Harris, R., & Major, J. (2017). Waves of destruction in the East Indies: The Wichmann catalogue of earthquakes and tsunami in the Indonesian region from 1538 to 1877. *Geological Society, London, Special Publications*, *441*(1), 9–46. https://doi.org/10.1144/SP441.2.

Heidarzadeh, M., Krastel, S., & Yalciner, A. C. (2014). The state-of-the-art numerical tools for modeling landslide tsunamis: A short review. In S. Krastel, et al. (Eds.), *Submarine mass movements and their consequences* (pp. 483–495). Cham: Springer.

Honthaas, C., Réhault, J. P., Maury, R. C., Bellon, H., Hémond, C., Malod, J. A., et al. (1998). A neogene back-arc origin for the Banda Sea basins: Geochemical and geochronological constraints from the Banda ridges (East Indonesia). *Tectonophysics*, *298*(4), 297–317. https://doi.org/10.1016/S0040-1951(98)00190-5.

Horspool, N., Pranantyo, I., Griffin, J., Latief, H., Natawidjaja, D., Kongko, W., et al. (2014). A probabilistic tsunami hazard assessment for Indonesia. *Natural Hazards and Earth System Sciences*, *14*(11), 3105–3122. https://doi.org/10.5194/nhess-14-3105-2014.

Imamura, F., Synolakis, C. E., Gica, E., Titov, V., Listanco, E., & Lee, H. J. (1995). Field survey of the 1994 Mindoro Island, Philippines tsunami. *Pure and Applied Geophysics*, *144*(3), 875–890. https://doi.org/10.1007/BF00874399.

Irsyam, M., Cummins, P., Asrurifak, M., Faisal, L., Natawidjaja, D., Widyantoro, S., et al. (2019). *Development of the 2017 national seismic hazard maps of Indonesia*. Earthquake Spectra. In press.

Irsyam, M., Sengara, I., Aldiamar, F., Widyantoro, S., Triyoso, W., Natawidjaja, D., Kertapati, E., Meilano, I., Suhardjono, Asrurifak, M., & Ridwan, M. (2010). Summary of study: Development of seismic hazard maps of Indonesia for revision of hazard map in SNI 03-1726-2002. Technical Report, Team for Revision of Seismic Hazard Maps of Indonesia, Bandung.

Jamelot, A., Gailler, A., Heinrich, P., Vallage, A., & Champenois, J. (2019). Tsunami simulations of the Sulawesi Mw 7.5 event: Comparison of seismic sources issued from a tsunami warning context versus post-event finite source. *Pure and Applied Geophysics*, *176*(8), 3351–3376. https://doi.org/10.1007/s00024-019-02274-5.

Kanamori, H., & Anderson, D. L. (1975). Theoretical basis of some empirical relations in seismology. *Bulletin of the Seismological Society of America*, *65*(5), 1073–1095.

Latief, H., Kodijat, A., Ismoyo, D., Bustamam, B., Adyasar, D., Nurbandika, N., & Rahayu, H. (2016). Air turun naik di tiga negeri. United Nations Educational, Scientific, and Cultural Organization, Office Jakarta - Indian Ocean Tsunami Information Centre, in Indonesian

Løvholt, F., Kühn, D., Bungum, H., Harbitz, C. B., & Glimsdal, S. (2012). Historical tsunamis and present tsunami hazard in eastern Indonesia and the southern Philippines. *Journal of Geophysical Research: Solid Earth*, *117*(B9), B09310. https://doi.org/10.1029/2012JB009425.

McCaffrey, R. (1988). Active tectonics of the eastern Sunda and Banda arcs. *Journal of Geophysical Research: Solid Earth*, *93*(B12), 15163–15182. https://doi.org/10.1029/JB093iB12p15163.

Okada, Y. (1985). Surface deformation due to shear and tensile faults in a half-space. *Bulletin of the Seismological Society of America*, *75*(4), 1135–1154.

Okal, E. A., & Reymond, D. (2003). The mechanism of great Banda Sea earthquake of 1 February 1938: Applying the method of preliminary determination of focal mechanism to a historical event. *Earth and Planetary Science Letters*, *216*(1–2), 1–15. https://doi.org/10.1016/S0012-821X(03)00475-8.

Okal, E. A., & Synolakis, C. E. (2004). Source discriminants for near-field tsunamis. *Geophysical Journal International*, *158*(3), 899–912. https://doi.org/10.1111/j.1365-246X.2004.02347.x.

Pairault, A. A., Hall, R., & Elders, C. F. (2003). Structural styles and tectonic evolution of the Seram Trough, Indonesia. *Marine and Petroleum Geology*, *20*(10), 1141–1160. https://doi.org/10.1016/j.marpetgeo.2003.10.001.

Patria, A., & Hall, R. (2017). The origin and significance of the seram trough, Indonesia.

Patton, J., Stein, R., & Sevilgen, V. (2018). Sunda Strait tsunami launched by sudden collapse of Krakatau volcano into the sea. *Temblor*. https://doi.org/10.32858/temblor.001.

Pownall, J., Hall, R., & Watkinson, I. (2013). Extreme extension across Seram and Ambon, eastern Indonesia: Evidence for Banda slab rollback. *Solid Earth*, *4*(2), 277–314. https://doi.org/10.5194/se-4-277-2013.

Pownall, J., Hall, R., & Lister, G. (2016). Rolling open Earth's deepest forearc basin. *Geology*, *44*(11), 947–950. https://doi.org/10.1130/G38051.1.

Pranantyo, I. R., & Cummins, P. R. (2019). Multi-data-type source estimation for the 1992 flores earthquake and tsunami. *Pure and Applied Geophysics*, *176*(7), 2696–2983. https://doi.org/10.1007/s00024-018-2078-4.

Rumphius, G. E. (1675). *Waerachtigh Verhael van de Schuckelijcke Aerdbebinge*. Dutch East Indies: BATAVIA.

Rumphius, G. E. (1997). True History of the terrible earthquake. (W. Buijze, translated by Beekman, E.M. and Foss, F. from (1675).

Sassa, S., & Takagawa, T. (2019). Liquefied gravity flow-induced tsunami: First evidence and comparison from the 2018 Indonesia Sulawesi earthquake and tsunami disasters. *Landslides*, *16*(1), 195–200. https://doi.org/10.1007/s10346-018-1114-x.

Soloviev, S., & Go, C. N. (1974). *Catalog of tsunamis in western coast of the Pacific Ocean* (pp. 1–30). Moscow: Academy of Sciences, USSR, Izdat Nauka.

Soloviev, S., Go, C., & Kim, X. (1986). *Catalog of tsunamis in the Pacific Ocean, 1969–1982* (p. 163). Moscow: MGC.

Spakman, W., & Hall, R. (2010). Surface deformation and slab-mantle interaction during Banda arc subduction rollback. *Nature Geoscience*, *3*(8), 562. https://doi.org/10.1038/NGEO917.

Synolakis, C. E. (1991). Green's law and the evolution of solitary waves. *Physics of Fluids A: Fluid Dynamics*, *3*(3), 490–491. https://doi.org/10.1063/1.858107.

Synolakis, C. E., Bardet, J. P., Borrero, J. C., Davies, H. L., Okal, E. A., Silver, E. A., et al. (2002). The slump origin of the 1998 Papua New Guinea tsunami. *Proceedings of the Royal Society of London Series A: Mathematical, Physical and Engineering Sciences*, *458*(2020), 763–789. https://doi.org/10.1098/rspa.2001.0915.

Watkinson, I. M., & Hall, R. (2017). Fault systems of the eastern Indonesian triple junction: Earth'svaluation of Quaternary activity and implications for seismic hazards. *Geological Society, London, Special Publications*, *441*(1), 71–120. https://doi.org/10.1144/SP441.8.

Wells, D. L., & Coppersmith, K. J. (1994). New empirical relationships among magnitude, rupture length, rupture width, rupture area, and surface displacement. *Bulletin of the Seismological Society of America*, *84*(4), 974–1002.

Wichmann, A. (1918). *Die Erdbeben Des Indischen Archipels Bis Zum Jahre 1857*. Amsterdam: Joahnnes Muller.

Wichmann, A. (1922). *Die Erdbeben Des Indischen Archipels von 1858 bis 1877*. Amsterdam: Uitgave van de Koninklijke Akademie van Wetenschappen.

(Received July 5, 2019, revised September 24, 2019, accepted December 5, 2019, Published online December 17, 2019)